A HIGH REYNOLDS NUMBER NUMERICAL SOLUTION OF THE NAVIER-STOKES EQUATIONS IN STREAM FUNCTION-VORTICITY FORM

By

JOHN H. BEARDEN

A Thesis
Submitted to the Faculty of
Mississippi State University
in Partial Fulfillment of the Requirements
for the Degree of Master of Science
in the Department of Aerophysics and
Aerospace Engineering

Mississippi State, Mississippi

August, 1977

A HIGH REYNOLDS NUMBER NUMERICAL SOLUTION OF THE NAVIER-STOKES EQUATIONS IN STREAM FUNCTION-VORTICITY FORM

By

JOHN H. BEARDEN

A Thesis
Submitted to the Faculty of
Mississippi State University
in Partial Fulfillment of the Requirements
for the Degree of Master of Science
in the Department of Aerophysics and
Aerospace Engineering

Mississippi State, Mississippi

August, 1977

A HIGH REYNOLDS NUMBER NUMERICAL SOLUTION OF THE NAVIER-STOKES EQUATIONS IN STREAM FUNCTION-VORTICITY FORM

by

John H. Bearden

Approved:

Professor of Aerospace Engineering and Head, Department of Aerophysics and Aerospace Engineering	Director of Graduate Instruction, College of Engineering
Professor of Aerophysics and Aerospace Engineering (Major Professor)	Dean of the College of Engineering

Dean of the Graduate School

August, 1977

ACKNOWLEDGEMENT

The support of NASA, Langley Research Center under Grant NCR-25-001-055 is gratefully acknowledged.

ABSTRACT

John H. Bearden, Master of Science, 1977

Major: Aerospace Engineering, Department of Aerophysics and Aerospace Engineering

Title of Thesis: A High Reynolds Number Numerical Solution of the Navier-Stokes Equations in Stream Function-Vorticity Form

Directed by: Dr. J. F. Thompson

Pages in Thesis: 49 Words in Abstract: 149

ABSTRACT

High Reynolds number, incompressible flow has posed many problems, some seemingly insurmountable, to researchers investigating this phenomenon. It will be the purpose of this investigation to consider what has been done in this field, and use this as a basis to attempt to overcome these problems and achieve a simulation of incompressible high Reynolis number flow.

A choice was made to use the stream function-vorticity form of the Navier-Stokes equations. The coordinate system used was a body fitted coordinate system with a "U" shaped outer boundary. A modified version of a numerical solution computer program was used to actually solve the Navier-Stokes equations around the body used in the research.

The particular body used in the investigation was an NACA-0018 airfoil. There was only moderate success, though, in this

simulation of flow at a Reynolds number of 1,000,000 and body angle-of-attack of zero.

TABLE OF CONTENTS

LIST OF FIGURES

LIST OF SYMBOLS

C_1	Difference equation coefficient
C_2	Difference equation coefficient
C_3	Difference equation coefficient
C_4	Difference equation coefficient
C_5	Difference equation coefficient
f(z)	Arbitrary function of z
i	Denotes position in the ξ η plane
JMAX	Denotes the maximum valve that the i index can attain
j	Denotes η position in the ξ η plane
k	Denotes position in non-dimensional time
p	Dimensional pressure
P	Contraction term of coordinate generation equation
Q	Contraction term of coordinate generation equation
R_0	Free stream Reynolds number
t	Dimensional time
u	Dimensional velocity in the x direction
v	Dimensional velocity in the y direction
x	Physical coordinate
y	Physical coordinate
α	Coordinate transformation parameter
β	Coordinate transformation parameter
γ	Coordinate transformation parameter
Γ_1	Body surface in the transformed plane
Γ_2	Outer boundary opposing the body surface in the transformed plane

Γ_3 Left reentrant boundary in the transformed plane

Γ_4 Right reentrant boundary in the transformed plane

Γ_5 Left infinity boundary in the transformed plane (only used in "U" shaped coordinate system)

Γ_6 Right infinity boundary in the transformed plane

δ Acceleration parameter

Δ Time increment used in the solution

η Nondimensional natural coordinate

υ Fluid kinematic viscousity, $ft^2/sec.$

ξ Non-dimensional natural coordinate

ρ Fluid density

σ Coordinate transformation parameter

τ Coordinate transformation parameter

ψ Non-dimensional stream function

ω Non-dimensional vorticity

Subscripts

i,j Denotes field position in the (ξ,η) plane

x First partial with respect to x

xx Second partial with respect to x

y First partial with respect to y

yy Second partial with respect to y

η First partial with respect to η

$\eta\eta$ Second partial with respect to η

ξ First partial with respect to ξ

$\xi\xi$ Second partial with respect to ξ

CHAPTER I

INTRODUCTION

Since modern computers made the numerical solution of the Navier-Stokes equations practical, the goal of researchers in the incompressible flow regime has been to simulate flow at high Reynolds numbers. The problems facing the researchers have proved to be excessive computer storage requirements as well as tremendous amounts of computer time needed. The computer storage requirement stems from the need for having very closely spaced coordinate lines in the field over which the solution is made because of the high Reynolds number flow. The necessity of using great quantities of computer time is caused by the use of extremely small time steps in the solution to maintain stability. Presented here is an approach to overcome at least part of these problems, and in doing so, achieve an accurate simulation of high Reynolds number flow about an airfoil.

There have already been computer programs written that solve the Navier-Stokes equations about arbitrary bodies that work well at low Reynolds numbers, so one of these was used as a basis for this work. Also, a "U" shaped coordinate system has been developed for use at high Reynolds numbers which was used. The difficulties faced in the research were the conversion of the computer program that solved the Navier-Stokes equations to a form compatible with the "U" shaped coordinate system, the experimental evaluation of the various acceleration parameters, and the determination of the body vorticity such that the body velocity would be zero. The work herein was done in

the stream function-vorticity form of the Navier-Stokes equations.

A very thorough discussion of the actual computational aspects and the computer code is contained in Reference [1]; this work by Thames has proved to be the backbone of this research. Also of possible interest to the reader is work by R. N. Reddy. This work by Reddy is also in the high Reynolds number range, but was done in the integro-differential form.[2] Work has also been done on submerged hydrofoils by S. P. Shanks. Shanks's research produced a computer code to simulate the flow around a submerged hydrofoil, both with and without bottom effects.[3]

CHAPTER II

ANALYTIC DEVELOPMENT

Due to the nature of this research, it might be advantageous to take a brief look at the derivation of the stream function-vorticity form of the Navier- Stokes equations and the transformation of these equations into the ψ,ω form for use in the transformed plane. A limited discussion of the related boundary conditions might also prove helpful.

In cartesian coordinates, the Navier-Stokes equations for non-steady, incompressible flow are:

$$u_x + v_y = 0, \qquad [\ 1.1a\ ]$$

$$u_t + u\,u_x + v\,u_y = -\frac{1}{\rho}p_x + \nu\nabla^2 u, \qquad [\ 1.1b\ ]$$

$$v_t + u\,v_x + v\,v_y = -\frac{1}{\rho}p_y + \nu\nabla^2 v, \qquad [\ 1.1c\ ]$$

where u and v are the velocity components in the x and y directions, respectively, where the subscripts represent partial differentiation with respect to the variable used, and where p is the pressure. These equations are transformed to the stream function-vorticity form by first defining:

$$u = \psi_y,\ v = -\psi_x,\ \omega = v_x - u_y; \qquad [\ 1.2a,b,c\ ]$$

then taking the curl of the Navier-Stokes equations, we have

$$\omega_t + \psi_y\,\omega_x - \psi_x\,\omega_y = \nu\nabla^2\omega, \qquad [\ 1.3a\ ]$$

$$\nabla^2\psi = -\omega, \qquad [\ 1.3b\ ]$$

With this information, the next step will be to consider the transformation of the stream function-vorticity equations from the

form used in the physical plane to that used on the rectangular transformed plane. The equations are transformed using the following operators:

$$f_x \equiv (y_\eta f_\xi - y_\xi f_\eta) / J \qquad [2.4a]$$

$$f_y \equiv (x_\xi f_\eta - x_\eta f_\xi) / J \qquad [2.4b]$$

And upon utilizing these operators the following equations result:

$$\omega_t + (\psi_\eta \omega_\xi - \psi_\xi \omega_\eta) / J =$$
$$(\alpha \omega_{\xi\xi} - 2 \beta \omega_{\xi\eta} + \gamma \omega_{\eta\eta} + \sigma \omega_\eta + \tau \omega_\xi) / J^2 R_0, \qquad [2.5a]$$
$$\alpha \psi_{\xi\xi} - 2 \beta \psi_{\xi\eta} + \gamma \psi_{\eta\eta} + \sigma \psi_\eta + \tau \psi_\xi = - J^2 \omega, \qquad [2.5b]$$

where the functions ω and ψ are doubly differentiable. The derivation of these expressions appears in Appendix A of Reference [1]. The coordinate system parameters α, β, γ, σ, τ, and J are:

$$\alpha \equiv x_\eta^2 + y_\eta^2,$$

$$J \equiv x_\xi y_\eta - x_\eta y_\xi,$$

$$\beta \equiv x_\xi x_\eta + y_\xi y_\eta,$$

$$\gamma \equiv x_\xi^2 + y_\xi^2$$

$$\sigma \equiv [y_\xi (\alpha x_{\xi\xi} - 2 \beta x_{\xi\eta} + \gamma x_{\eta\eta}) - x_\xi (\alpha y_{\xi\xi} - 2 \beta y_{\xi\eta} + \gamma y_{\eta\eta})] / J$$

$$\tau \equiv [x_\eta (\alpha y_{\xi\xi} - 2 \beta y_{\xi\eta} + \gamma y_{\eta\eta}) - y_\eta (\alpha x_{\xi\xi} - 2 \beta x_{\xi\eta} + \gamma x_{\eta\eta})] / J$$

Note that the Equations [2.5a,b] have been non-dimensionalized with respect to the free-stream velocity and the airfoil chord. The Reynold's number, R_o, is also based on these quantities.

In the case under consideration, where the coordinate system remains fixed in time, the coordinate system parameters must only be calculated once since they remain constant throughout the solution. Also, if the coordinate system has no contraction of the coordinate lines about the body, the coordinate system parameters σ and τ disappear.

The boundary conditions for the equations in the rectangular transformed plane are expressed in the following relations:

$$\psi(x,y,t) = \psi_\infty(x,y,t) \ , \ x,y \in \Gamma_2 \qquad [2.7a]$$

$$\omega(x,y,t) = \omega_\infty(x,y,t) \ , \ x,y \in \Gamma_2 \qquad [2.7b]$$

$$\psi(x,y,t) = \psi_0 = \text{constant}, \ y,y \in \Gamma_1 \qquad [2.7c]$$

$$\frac{\partial \psi}{\partial \underset{\sim}{n}^{(\Gamma_1)}} (x,y,t) = 0, \ [x,y] \in \Gamma_1 \qquad [2.7d]$$

where Γ_1 and Γ_2 are the body and the outer boundary line segments, respectively. Equation [2.7d] specifies conditions that, if met, guarantee the tangential velocity on the body surface to be zero. Since the normal component vanishes in the same manner, it can be assumed that the no-slip boundary conditions are met by satisfying this equation.

For a much more indepth discussion on the material presented here the reader is to refer to Reference [1]. Here Thames covers the various aspects required in setting up the boundary conditions, as well as, the transformations used in manipulating the equations.

CHAPTER III

THE COORDINATE SYSTEM

The coordinate system used in this work is a body fitted coordinate system, that is, one that fits one coordinate line through every point specified on the body being considered. This type of coordinate line will be called an η-line. Another η-line is then fitted to the outer boundary and the remaining lines spaced throughout the field. A second type of lines is then used to subdivide the η-lines, referred to here as ξ-lines. Although the coordinate system created by this method is not necessarily orthogonal, there are no severe problems caused. On the contrary, the fact that the coordinate lines follow the body contour, thus eliminating any extrapolation, produces a profound advantage in the accuracy provided in the boundary layer. References [1], [4], [5], and [6] cover this topic in greater detail.

Figure [1] shows such a coordinate system, in this case an airfoil in an elliptical outer boundary. Also, Figure [2] shows the rectangular transformed plane. This transformed plane is created by "opening up" the body fitted coordinate system from the cut. The line segment Γ_1 in the body fitted coordinate system is analogous to Γ_1^* in the transformed plane. the same correspondence also carries for Γ_2 and Γ_2^*, as well as for Γ_3 and Γ_3^* and Γ_4 and Γ_4^*. Note that Γ_3 and Γ_4 are colinear, therefore each point on Γ_3^* is equal to the corresponding point on Γ_4^*.

By starting with some initial guess, Figure [3], the body

fitted coordinate system is generated by solving two elliptic partial differential equations that have Dirichlet boundary conditions. These equations are:

$$\xi_{xx} + \xi_{yy} = P(\xi, \eta), \qquad [3.1a]$$

$$\eta_{xx} + \eta_{yy} = Q(\xi, \eta), \qquad [3.1b]$$

with one coordinate being set constant on the body and outer boundary and the other varying monotonically around the body. Since the initial guess specifies the values of x and y for each ξ,η point, the dependent and independent variables in the equations must be interchanged. Upon doing this, they take on the form of:

$$\alpha x_{\xi\xi} - 2\beta x_{\xi\eta} + \gamma x_{\eta\eta} = -J^2 \left(x_\xi P(\xi, \eta) + x_\eta Q(\xi,\eta) \right) \qquad [3.2a]$$

$$\alpha y_{\xi\xi} - 2\beta y_{\xi\eta} + \gamma y_{\eta\eta} = -J \left(y_\xi P(\xi, \eta) + y_\eta Q(\xi,\eta) \right) \qquad [3.2b]$$

This quasi-linear elliptic set of partial differential equations is much more complex than the linear equations [3.1], but the boundary conditions are specified at the body and outer boundary which are straight lines in the rectangular transformed plane. Also, the grid spacing in the transformed plane is unity. The inhomogeneous terms in equations [3.2], $P(\xi,\eta)$ and $Q(\xi,\eta)$, are used in the contraction of the η-lines to the body, to a given line, or even to some specified point. These terms are derived from the sums of decaying exponentials. Further discussion of this topic is contained in Reference [6].

These equations are then solved over the rectangular transformed plane using central space differences and successive overrelaxation

iteration.

With this as a basis, the coordinate system used in this research will be considered. Instead of enclosing the body, in this case an airfoil, in an elliptical outer boundary, it is enclosed in a "U" shaped outer boundary, Figure [4]. The reasons for doing this are the high contraction requirements and the necessity for good grid resolution in the wake. For high Reynolds number flow, the coordinate lines must be contracted very closely to the body to get enough lines in the boundary layer to manitain stability in the solution. This creates problems, though, in that the lines that are contracted close to the body, in the system with an elliptical outer boundary, must bend around the sharp trailing edge. This bend brings the lines so close together that the separation becomes the order of magnitude of the roundoff error. But with the "U" shaped coordinate system, the η-lines "flow" off of the trailing edge completely eliminating this problem, Figure [6]. Also, the system with an elliptical outer boundary does not have sufficient lines in the wake area downstream of the body, and the lines spread out even more further downstream. The "U" shaped coordinate system also alleviates this problem because of the flow of the lines from the trailing edge. Note, also, that the lines have very little spread downstream of the body. This gives excellent resolution in the wake. This type of system is created in the same manner as the type with the elliptical outer boundary. The major difference is the way the rectangular transformed plane is set up, with the body and the reentrant segments

on the ξ=1 line and the infinity boundary occupying the other three sides. Referring to Figure [4] and Figure [5], some idea of the nature of the correspondence of the physical plane to the transformed plane may be gained. Again, Γ_1 in the physical plane is the same as the Γ_1^* line segment in the transformed plane and Γ_2 corresponds to Γ_2^*, Γ_3 to Γ_3^*, and so on. Since the coordinate lines Γ_3^* and Γ_4^* in the transformed plane represent the "cut" in the physical plane, they require special treatment when calculating the derivative across the "cut." Consider a point on Γ_2^* that has coordinates (N,1), where $1 < N < LBY1$, and where LBY1 is the left hand coordinate of the body. It's corresponding point on Γ_3^* then has the coordinates [IMAX - (N-1), 1], where IMAX is the number of ξ-lines in the field. Using this, the derivative of ψ with respect to η becomes:

$$\psi_\eta = \psi_{N,2} - \psi_{IMAX-(N-1),2}$$

In the same manner the partial derivative of ω with respect to ξ and η becomes:

$$\omega_{\xi\eta} = \omega_{N+1,2} - \omega_{IMAX-(N-2),2} + \omega_{IMAX-N,2} - \omega_{N-1,2}$$

instead of the form used in the field calculations which is:

$$\omega_{\xi\eta} = \omega_{i+1,\ j+1} - \omega_{i+1,\ j-1} + \omega_{i-1,\ j-1} - \omega_{i-1,\ j+1}$$

This holds true for all derivatives taken across the cut.

The coordinate system was generated using the TOMCAT code in Reference [6]. The code permits the attraction of the lines to decay aft of the trailing edge thus permitting them to expand slightly, this feature was also used in research. The outer boundary was set up 5

chord lengths from the body except for the downstream dimension which was 10. The coordinate system has 10 coordinate lines contracted into the boundary layer, this attraction is explained in the appendix, Figure [6].

CHAPTER IV

THE NUMERICAL SOLUTION PROGRAM

Perhaps the next step would be an explanation of the computer code used in this research to solve the Navier-Stokes equations over the rectangular transformed plane. This code was written by F. C. Thames, [1] and was chosen for the work because it uses the stream function-vorticity form of the Navier-Stokes equations.

The space derivatives of this solution are approximated using central differences and the vorticity time derivatives using a first-order backward time difference. This implicit numerical method with SOR iteration is used to converge the space derivative variations in the flow solution. Then, with the field converged, the vorticity on the body is approximated with modified false position iteration. This method of iterating the body vorticity is designed to force the body tangential velocity to zero.[1][5][7][8]

The numerical procedures used in accomplishing the solution and the finite difference form of the Navier-Stokes equations are now given attention. The finite difference grid, that is the rectangular transformed plane, is pictured in Figure [7] for clarity. The grid pictured is one used in the "U" shaped coordinate system. The dark-circles represent the body, on the J=1 line, and the outer boundary on the I=1, I=IMAX, and J=JMAX lines. The points represented by the open circles are the re-entrant boundary segments and as pointed out earlier represent the same set of points in the physical plane. In

other words the point immediately down stream of the trailing edge in the physical plane is represented by the points I and II in the transformed plane, Figure [7]. Since the velocity at the outer boundary is the free stream velocity and the vorticity is zero and since the body velocity is zero, the boundary conditions are specified at all points denoted by a darkened circle in Figure [7].

The procedure used in solving the difference equations over the rectangular transformed coordinate system is central differencing for the spacial derivatives and backwards differencing for the time derivative of the vorticity. The difference equation for the vorticity, after substituting the central difference and backwards difference approximations, is:

$$(\omega^n_{i,j} - \omega^{n-1}_{i,j})/\Delta t = [(\psi'_\xi)^n_{i,j}(\omega'_\eta)^n_{i,j} - (\psi'_\eta)^n_{i,j}(\omega'_\xi)^n_{i,j}]/J'_{i,j}$$
$$+ 4[\alpha'_{i,j}(\omega'_{\xi\xi})^n_{i,j} - \beta'_{i,j}(\omega'_{\xi\eta})^n_{i,j}/2 + \gamma'_{i,j}(\omega'_{\eta\eta})^n_{i,j}$$
$$+ \sigma'_{i,j}(\omega'_\eta)^n_{i,j} + \tau'_{i,j}(\omega'_\xi)^n_{i,j}]/R_0(J'_{i,j})^2 \qquad [\ 4.1\ ]$$

where the primed quantities represent difference expressions documented in Appendix D of Reference [1]. Then solving for $\omega^n_{i,j}$ yields:

$$\omega^n_{i,j} = [(C'_1)_{i,j} - (C'_4)_{i,j}(\psi'_\eta)^n_{i,j} + (C'_6)_{i,j}]\omega^n_{i+1,j}$$
$$+ [(C'_1)_{i,j} + (C'_4)_{i,j}(\psi'_\eta)^n_{i,j} - (C'_6)_{i,j}]\omega^n_{i-1,j}$$
$$+ [(C'_3)_{i,j} + (C'_4)_{i,j}(\psi'_\xi)^n_{i,j} + (C'_5)_{i,j}]\omega^n_{i,j+1}$$
$$+ [(C'_3)_{i,j} - (C'_4)_{i,j}(\psi'_\xi)_{i,j} - (C'_5)_{i,j}]\omega^n_{i,j-1}$$
$$+ [(C'_2)_{i,j}](\omega'_{\xi\eta})^n_{i,j} + \{1 - 2[(C'_1)_{i,j} + (C'_3)_{i,j}]\}\omega^n_{i,j} \qquad [\ 4.2\ ]$$

where:

$$(C_1')_{i,j} \equiv 4\Delta t\alpha'_{i,j}/\Delta$$

$$(C_2')_{i,j} \equiv -2\Delta t\beta'_{i,j}/\Delta$$

$$(C_3')_{i,j} \equiv 4\Delta t\gamma'_{i,j}/\Delta$$

$$(C_4')_{i,j} \equiv \Delta t R_0 J'_{i,j}/\Delta$$

$$(C_5')_{i,j} \equiv 4\Delta t\sigma'_{i,j}/\Delta$$

$$(C_6')_{i,j} \equiv 4\Delta t\tau'_{i,j}/\Delta$$

and

$$\Delta = R_0(J'_{i,j})^2 + 8\Delta t(\alpha'_{i,j} + \gamma'_{i,j})$$

The stream function equation is derived in the same manner and is:

$$\begin{aligned} 2[(C_1')_{i,j} + (C_3')_{i,j}]\psi^n_{i,j} &= [(C_1')_{i,j} + (C_6')_{i,j}]\psi^n_{i+1,j} \\ &+ [(C_1')_{i,j} - (C_6')_{i,j}]\psi^n_{i-1,j} + [(C_3')_{i,j} + (C_5')_{i,j}]\psi^n_{i,j+1} \\ &+ [(C_3')_{i,j} - (C_5')_{i,j}]\psi^n_{i,j-1} + \Delta t\{1 - 2[(C_1')_{i,j} + (C_3')_{i,j}]\}\omega^n_{i,j}/R_0 \\ &+ [(C_2')_{i,j}](\psi'_{\xi\eta})^n_{i,j} \end{aligned} \qquad [\ 4.3\ ]$$

The vorticity and stream function equations are then solved simultaneously over the computational grid by SOR iteration at each time step. Also it is necessary to calculate the vorticity iterate first in each sweep of the field if the two equations are coupled.

As Thames points out, there are two observations that should be made about these difference equations. The first being the large quantities of computer storage needed for the implimentation of the solution. The reason being the nine field size arrays used to store the six coefficient arrays, the ψ array, and the ω^n and ω^{n-1} arrays.

Secondly, the fact that the velocity tangent to the body is explicitly enforced at zero alleviates instabilities in the solution.

The changes made in this computer code were centered around the change from a coordinate system with the elliptical outer boundary to one that has the "U" shaped outer boundary. Recall from Chapter III that the re-entrant segments were moved from the I=1 and I=IMAX lines in the transformed plane of the elliptical coordinate system to either side of the body on the J=1 line of the transformed plane of the "U" shaped coordinate system. Also the infinity boundary was moved to where it occupied the three remaining sides of the field of the "U" shaped coordinate system. Since no calculations are made on the infinity boundary, the original code swept the field from I=1 to I=IMAX and then from J=2 to J=JMAX-1. That is every point is swept except the body and the infinity boundary at J=JMAX. But on the "U" shaped system, with the infinity boundary on the I=1, I=IMAX, and the J=JMAX lines, the field must be swept from I=2 to I=IMAX-1 and J=2 to J=JMAX-1, or in ohter words, all the interior points of the field. Then the points on the re-entrant boundary segments had to be calculated. This was done by sweeping from I=2 to the point immediately down stream of the body. Note that the J=-1 points shown in Figure [8] correspond to the J=2 points of the other re-entrant segment. And, finally, the program was changed to sweep only the body points on the I=1 lines and not the entire line.

The body vorticity was calculated using Isreali's method for the first two changes in body vorticity. The algorithm is:

$$\omega_{i,1}^{(k+1)} = \omega_{i,1}^{(k)} - \delta \left(\frac{\partial \psi}{\partial n}\right)_{i,1}^{(k)}$$

But the method is slow and is therefore used only to make the first couple of changes in body vorticity. The subsequent iteration in body vorticity is done with the false position method:

$$\omega_{i,1}^{(k+1)} = \omega_{i,1}^{(k)} - \delta \frac{\omega_{i,1}^{(k)} - \omega_{i,1}^{(k-1)}}{\left[\frac{\partial \psi}{\partial \underset{\sim}{n}_1}\right]_{i,1}^{(k)} - \left[\frac{\partial \psi}{\partial \underset{\sim}{n}_1}\right]_{i,1}^{(k-1)}} \left[\frac{\partial \psi}{\partial \underset{\sim}{n}_1}\right]_{i,1}^{(k)}$$

Because the boundary condition is imposed on ψ and $\frac{\partial \psi}{\partial n}$, the vorticity, ω, is calculated such that the body velocity is zero. R. L. Walker also used this method in an investigation of flow over a semi-infinite flat plate, Reference [8].

CHAPTER V

RESULTS

The test case considered in this research was the flow about an NACA-0018 airfoil at a Reynolds number of 1,000,000. Detail of the coordinate system near the airfoil is shown in Figure [9]. The entire field is shown in Figure [6]. This case was run using a one-hundred step gradual start. The velocity was gradually increased by an increment of .01 from zero to free-stream velocity while holding the Reynolds number fixed at 1,000,000. The field vorticity acceleration parameter was 1.8, and the vorticity convergence tolerance, the stream function convergence tolerance, and the maximum body velocity were set at 0.0001, 0.00001, and 0.0001, respectively.

There were some difficulties encountered in starting the solution. The primary difficulty was finding an accurate approximation for the trailing edge vorticity. The cause of the problem appeared to be a loss of symmetry of the vorticity between the top and the bottom of the airfoil, probably due to the extreme gradients encountered in the start. The number of iterations required to converge the field was so large that the body velocity was converged to a value of .005 rather than .0001 during the start. Even with this change, it became necessary to ignore the value of velocity at the trailing edge points and the two points adjacent to the trailing edge. The vorticity at the trailing edge, then had to be set at zero rather than calculated because the velocity was not converged at the points used for extropolating the

vorticity. This is valid for a symmetric flow. Finally, just before the solution reached free-stream velocity, the assymmetry caused the solution to diverge. To correct this, the points above and below the airfoil were averaged to make the field symmetrical.

Once the solution reached free-stream velocity, the assymmetry was still present as shown in Figure [10] which pictures the streamlines around the airfoil at time step 110. Since this assymmetric vorticity distribution caused the solution to diverge, it had to be somehow eliminated. Refer to Figure [11] and Figure [12] which show the velocity distribution around the airfoil. Note that the velocity leaving the upper surface is greater than that leaving the lower surface, even at time step 20. This could be caused by one of two things, first, the relative field vorticity iteration error was only converged to a value of .001, rather than to .0001, before the first change in body vorticity was made, thus leading to error before the solution is even started. Secondly, the field and body numerical iteration scheme sweeps from the trailing edge around the under side of the airfoil then over the top of the airfoil and back to the trailing edge. It is possible that this method of "sweeping" the field is perhaps biasing the velocity around the body, as a result of the large gradients at the start, leading to a higher velocity on the top of the airfoil. Figure [13] shows the pressure distribution on the airfoil at four times. Due to the above-mentioned numerical error, the assymmetric pressure distribution becomes worse as time progresses. The pressure coefficient after the acceleration has stopped does, however, resemble the expected profile for this airfoil. The drag is about twice the experimental

value, but was still decreasing at the end of the run. The high drag and the linear tendency in the pressure distribution during the start are, of course, due to the acceleration.

Two proposed changes to correct these problems are: (1) Converge the field vorticity iteration error more completely before attempting a change in body vorticity. (2) Sweep the field from the center to the outside edges, i.e., leading edge to trailing edge rather than from left to right, and start from a potential flow.

APPENDIX

AUTOMATIC CONCENTRATION OF COORDINATE LINES INTO A BOUNDARY LAYER*

In this appendix, the procedure by which a specified number of coordinate lines can be automatically concentrated into a boundary layer of specified thickness is discussed. Consider the coordinate system generation equations (3.2) applied to the one-dimensional case of straight boundaries parallel to the x-axis. With η = constant on these boundaries, and the ξ-lines being normal to the boundaries, we have $Y_\xi = Y_{\xi\xi} = Y_{\xi\eta} = 0$ and the x-equation is identically zero so that the coordinate equations reduce to

$$\gamma Y_{\eta\eta} + J^2 Q Y_\eta = 0 \tag{A-1}$$

or

$$\frac{Y_{\eta\eta}}{Y_\eta} + \frac{J^2}{\gamma} Q = 0 \tag{A.2}$$

This can be made a perfect differential by choosing the form of the control function Q to be

$$Q(\eta) \equiv - \frac{\gamma}{J^2} \frac{f''(\eta)}{f'(\eta)} \tag{A.3}$$

where the minus sign has been introduced merely for convenience. Then (A.2) becomes

$$\frac{y''}{y'} - \frac{f''}{f'} = 0 \tag{A.4}$$

---

*Personal communication from Dr. Thompson

which can be integrated to yield

$$y(\eta) = c_1 f(\eta) + c_2 \tag{A.5}$$

The constants of integration may be evaluated from the boundary condition: $y(1) = y_1$, $y(J) = y_J$ so that

$$y(\eta) = y_1 + (y_J - y_1)\left(\frac{f(\eta) - f(1)}{f(J) - f(1)}\right) \tag{A.6}$$

This equation should be solved for $f(\eta)$ to yield

$$\frac{f(\eta) - f(1)}{f(J) - f(1)} = \frac{y(\eta) - y_1}{y_J - y_1} \tag{A.7}$$

which, with arbitrary definition of $f(1)$ and $f(J)$ will yield the required $f(\eta)$, and hence the required $Q(\eta)$ via substitution in (A.3), to produce a desired distribution $y(\eta)$. The evaluation of $Q(\eta)$ may be done without actual evaluation of $f(\eta)$, however, by solving (A.4) for y''/y' and substituting into (A.3) to produce

$$Q(\eta) = -\frac{\gamma}{J^2}\frac{y''}{y'} \tag{A.8}$$

Now a number of smooth functions for $y(\eta)$, such as exponentials, logarithmic functions, hyperbolic function, etc., may be found which will concentrate lines near y_1 with a spread out to y_2. However, since the boundary layer thickness at high Reynolds number is only a very small fraction of the distance to outer boundary of the computational field, such smooth functions cannot allow the lines to spread rapidly enough outside of the boundary layer. The result is that nearly all of the lines in the field will be within a few boundary layer thicknesses of the body, with a great gap near the outer boundary.

Therefore, a composite function was used for $y(\eta)$, formed by joining a logarithmic function to a quartic polynomial near the edge of the boundary layer. This function was constructed as follows: assume that it is desired to space the lines in the boundary layer such that the change in velocity from each at the next is the same. Let the velocity profile in the boundary layer be approximated by the exponential

$$u(y) = 1 - e^{-ey} \tag{A.9}$$

Let the edge of the boundary layer be defined by

$$u = 0.99 \text{ at } y = \delta$$

Then the decay factor c will be given by

$$c = -\frac{1}{\delta} \ln (0.01) \tag{A.10}$$

Now solve (A.9) for y(u):

$$y(u) = -\frac{1}{c} \ln (1-u) \tag{A.11}$$

In order to achieve the same velocity change from each line to the next, take $u = 0.99 \left(\frac{\eta-1}{\eta_\delta-1}\right)$ where η_δ is the line at the edge of the boundary layer. Substitution is (A.11) then yields

$$y(\eta) = -\frac{1}{c} \ln \left[1 - 0.99 \left(\frac{\eta-1}{\eta_\delta-1}\right)\right] \quad 1 \le \eta < \eta_\delta \tag{A.12}$$

Let this logarithmic function be joined to a quartic polynomial at some line inside or at the outer edge of the boundary layer. Thus with the function at $\eta=N$, the polynomial is of the form

$$y(\eta) = y'(N)\,[\eta-N] + \frac{1}{2} y''(N)\,[\eta-N]^2 + \frac{1}{6} y''(N)\,[\eta-N]^3 + a(\eta-N)^4 + y(N)$$

$$N \le \eta \le J \tag{A.13}$$

Here y'(N) is functional notation, etc. The derivatives are determined by differentiation of (A.12) with evaluation at η=N. The remaining coefficient "a" is used to satisfy the boundary condition at the outer boundary $y(J) = y_J$. Thus

$$a = \frac{y_J - y(N) - y'(N)\ [J-N] - \frac{1}{2}\, y''(N)\ [J-N]^2 - \frac{1}{6}\, y''(N)\ [J-N]^3}{(J-N)^4} \qquad (A.14)$$

Note that the junction to the polynomial need not occur at the edge of the boundary layer, but anywhere inside it. It was found advantageous to place the junction two or three lines inside the boundary layer.

Thus if the boundary layer thickness, δ, and the number of lines therein, η_δ, are specified, along with the distance to the outer boundary, y_J, and the total number of lines J, and the function line N, the control function $Q(\eta)$ can be evaluated from

$$Q(\eta) = -\frac{\gamma}{J^2} \frac{\frac{0.99}{\eta_\delta - 1}}{1 - 0.99\ (\frac{\eta-1}{\eta_\delta - 1})} \qquad \eta = 1,2,--,\ N \le \eta_\delta \qquad (A.15)$$

$$Q(\eta) = -\frac{\gamma}{J^2} \frac{y''(N) + y''(N)\ [\eta-N] + 12a[\eta-N]^2}{y'(N) + y''(N)\ [\eta-N] + \frac{1}{2}\, y''(N)\ [\eta-N]^2 + 4a[\eta-N]^3}$$

$$\eta = N,\ N+1,\ ---,\ J \qquad (A.16)$$

with the required derivatives given by

$$y^{(k)}\ (N) = \frac{\frac{(k-1)!}{c}\ (\frac{0.99}{N-1})^k}{[1 - 0.99\ (\frac{\eta-1}{N-1})]^k} \qquad k = 1,2,3 \qquad (A.17)$$

and y(N) by

$$y(N) = -\frac{1}{c} \ln[1 - 0.99\ (\frac{N-1}{\eta_\delta - 1})] \qquad (A.18)$$

Although this analysis is developed for the one-dimensional case of a flat boundary, much the same results will be achieved by its use with curved boundaries since curvature tends to affect both the boundary layer thickness and the line control in the same way. Thus convex curvature thins the boundary layer but also causes the lines to concentrate to a greater degree near the boundary.

In the present work, the boundary layer thickness was taken as $\delta = \frac{5}{\sqrt{R}}$ where R is the chord Reynolds number, and 10 lines were placed therein ($\eta_\delta = 10$) with the junction to the polynomial at line 7 (N = 7). There were 31 lines in the field, and the outer boundary was at 5 ($J = 31$, $y_J = 5$).

Additional coordinate system control, in the form of ξ-line attraction was used to pool the ξ-lines in the wake nearer the trailing edge. This attraction was of the exponential type used in Thames [1] and in the original TOMCAT code [6], except that in order to be compatible with the boundary layer attraction function, the attraction was calculated for

$$Q(\eta) = -\frac{1}{J^2} S(\eta) \qquad (A.19)$$

where $S(\eta)$ corresponds to the $Q(\eta)$ of [1] and [6]. The attraction was point attraction to the trailing edge, with amplitude of 0.7 on the bottom of the trailing edge and -0.7 on the top. The decay factor was 0.1 and the feature of attraction to the convex side and repulsion to the concave provided for in the TOMCAT code was activated.

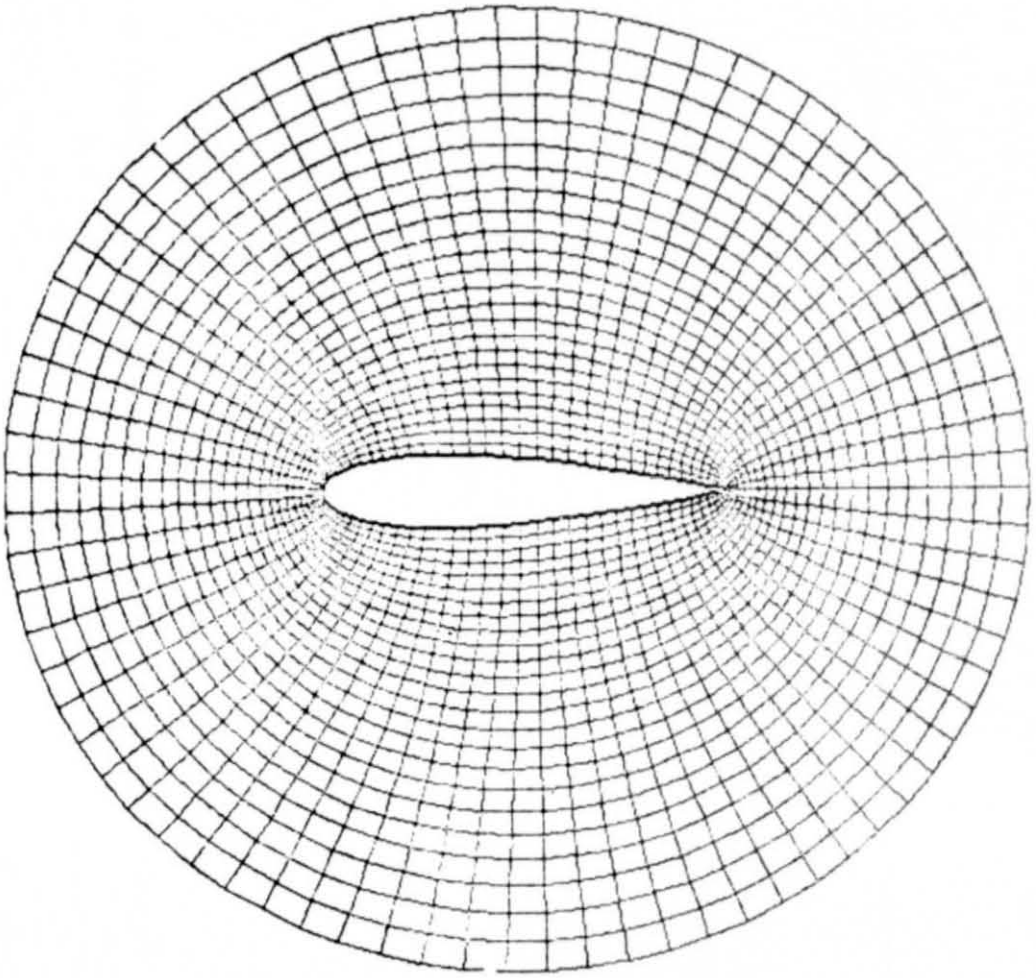

Figure 1. Coordinate System - Elliptical Outer Boundary

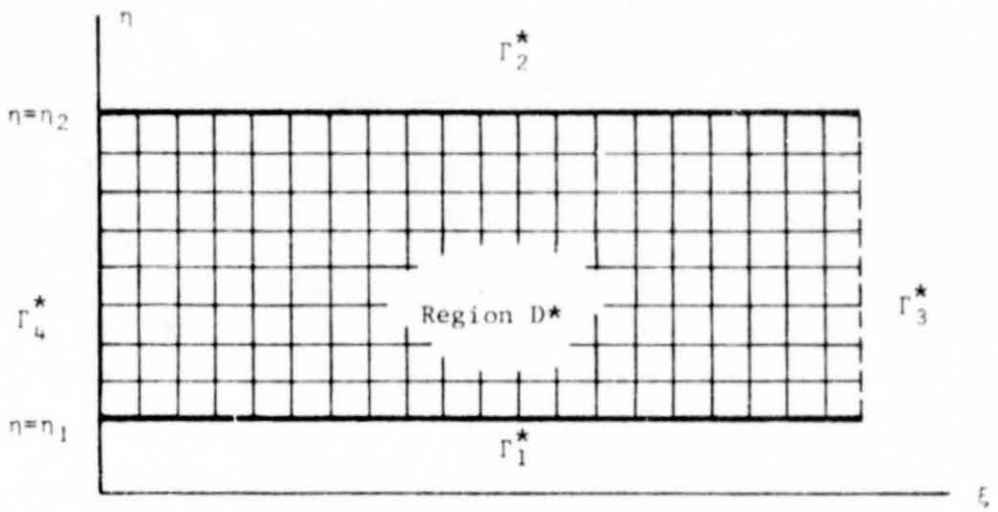

Transformed Plane
(Natural Coordinates)

Figure 2. Transformed Plane - Elliptical Outer Boundary

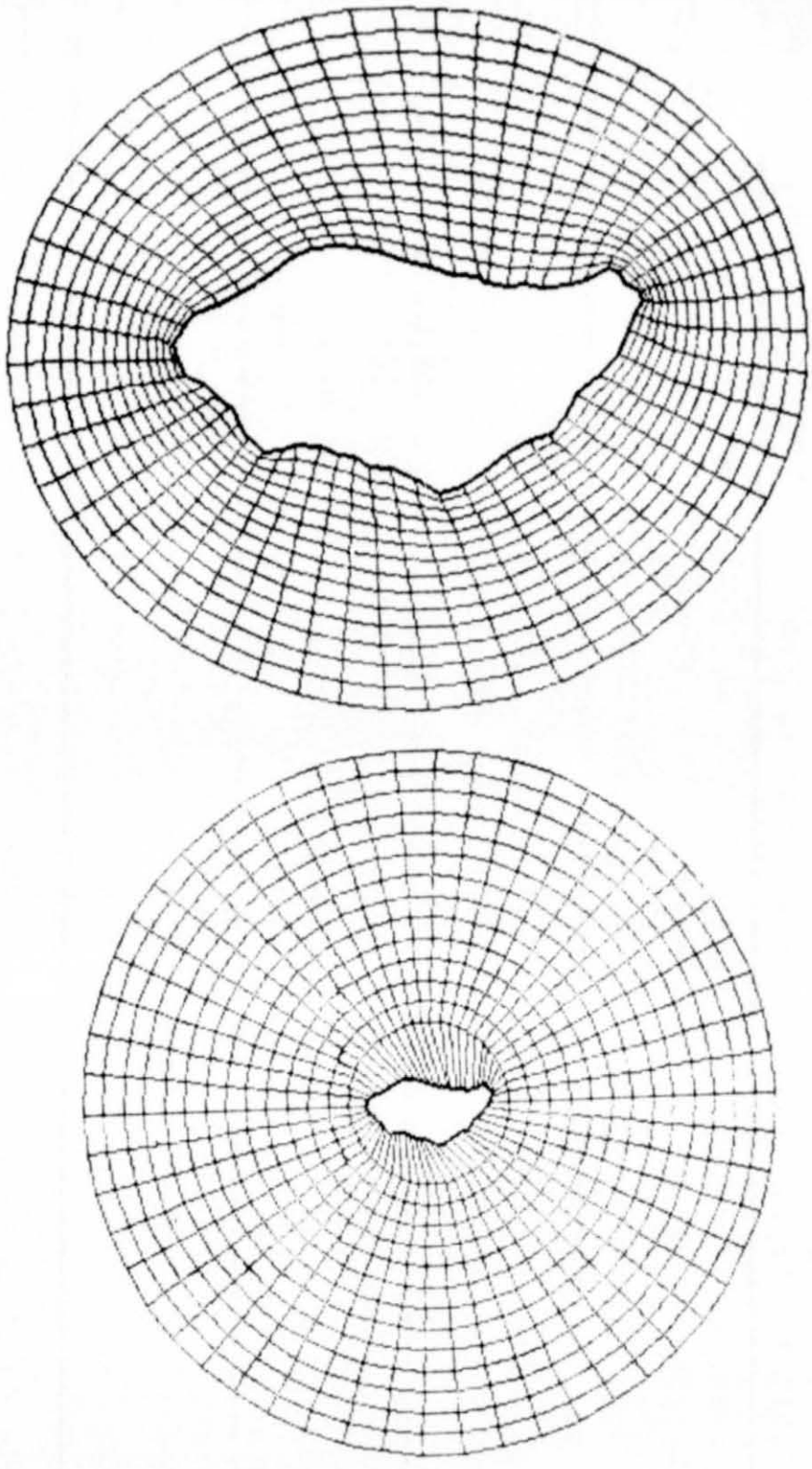

Figure 3. Initial Guess for Coordinate Generation

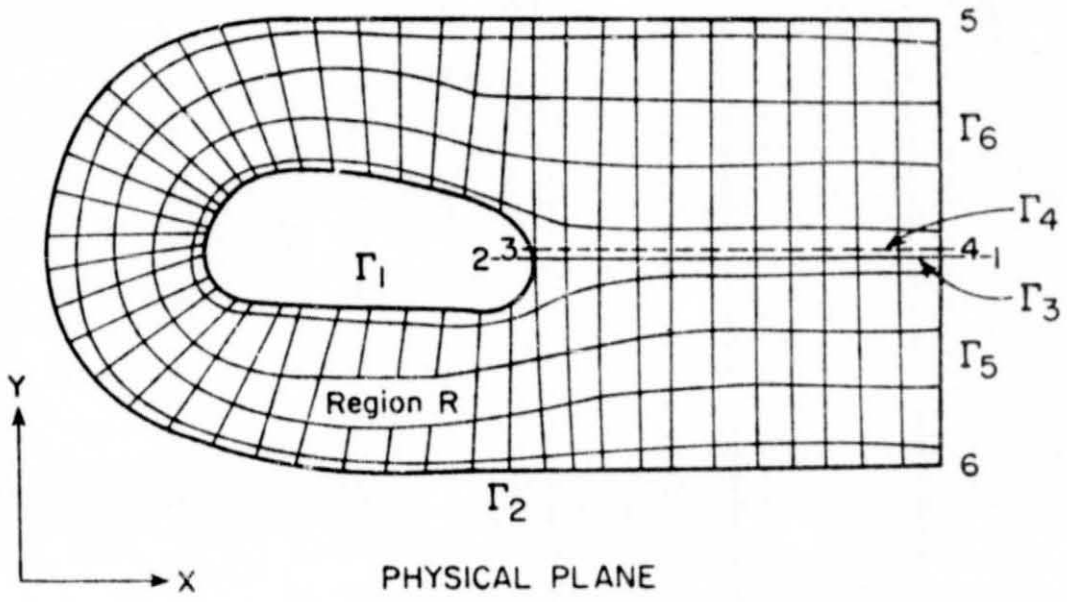

Figure 4. Coordinate System - "U" Shaped Outer Boundary

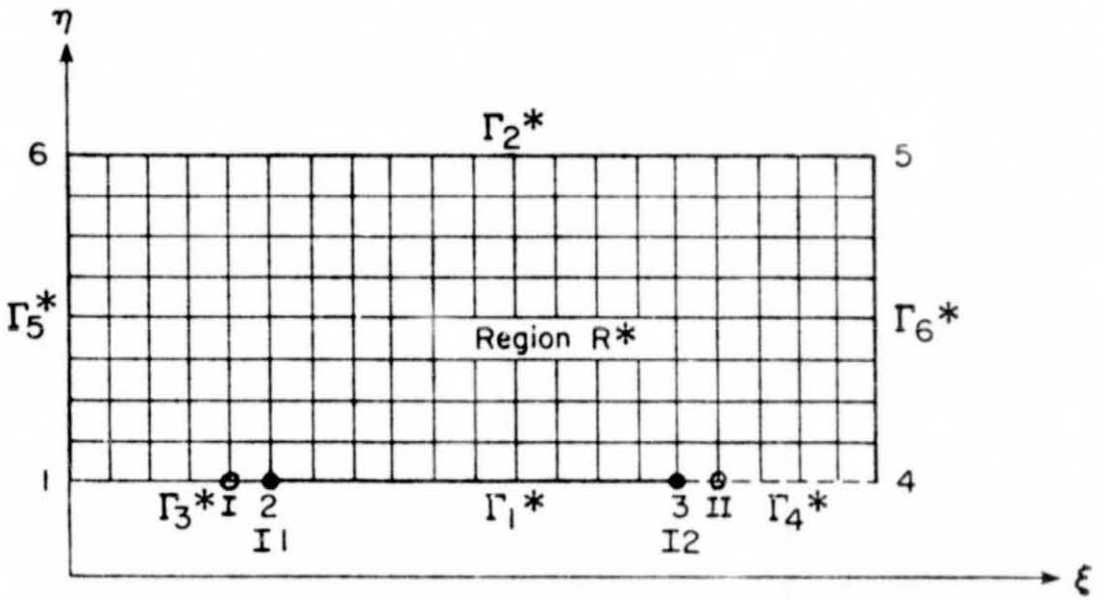

RECTANGULAR TRANSFORMED PLANE
(NATURAL COORDINATES)

Figure 5. Coordinate System Transformed Plane -
"U" Shaped Outer Boundary

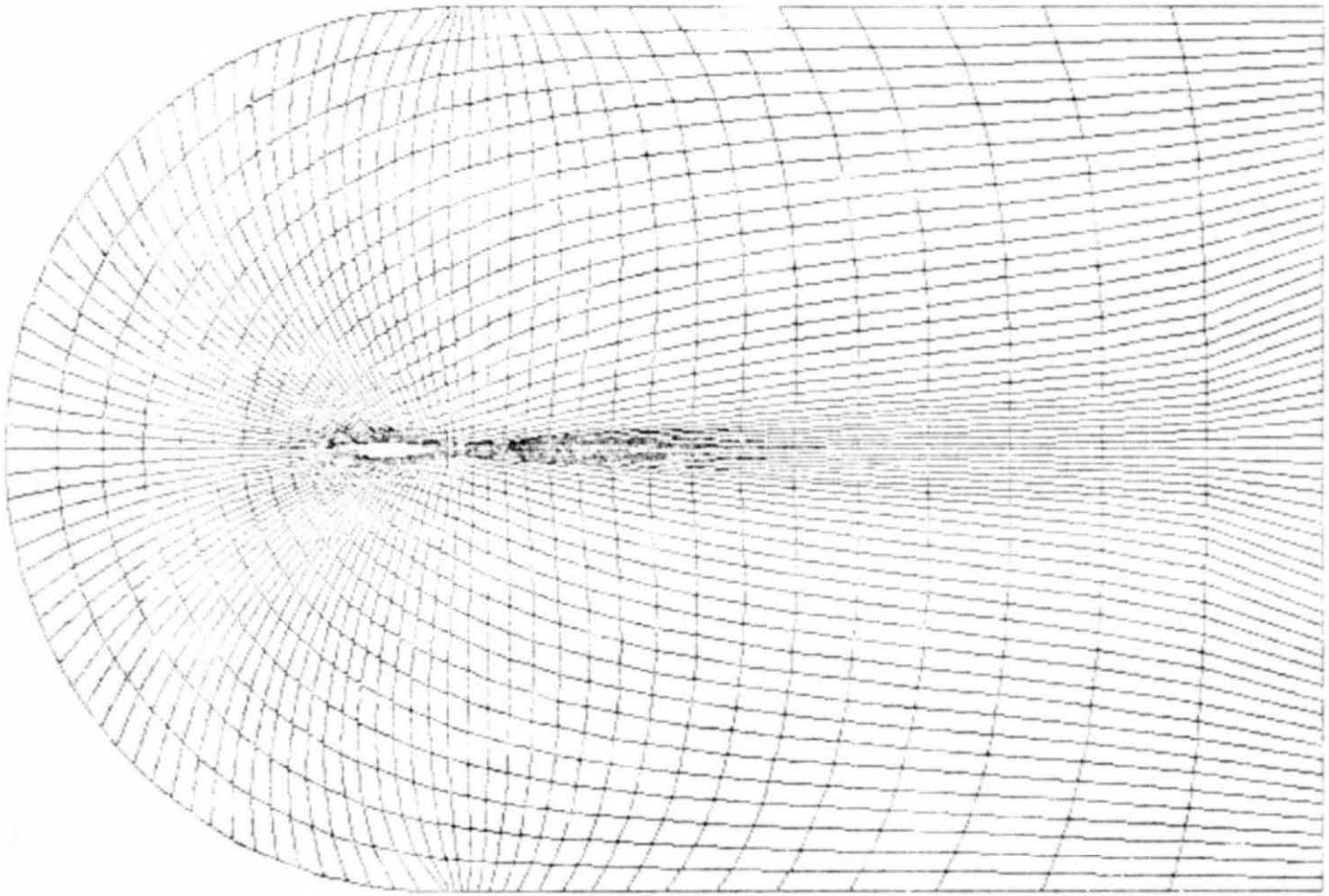

Figure 6. Coordinate System Used in the Solution

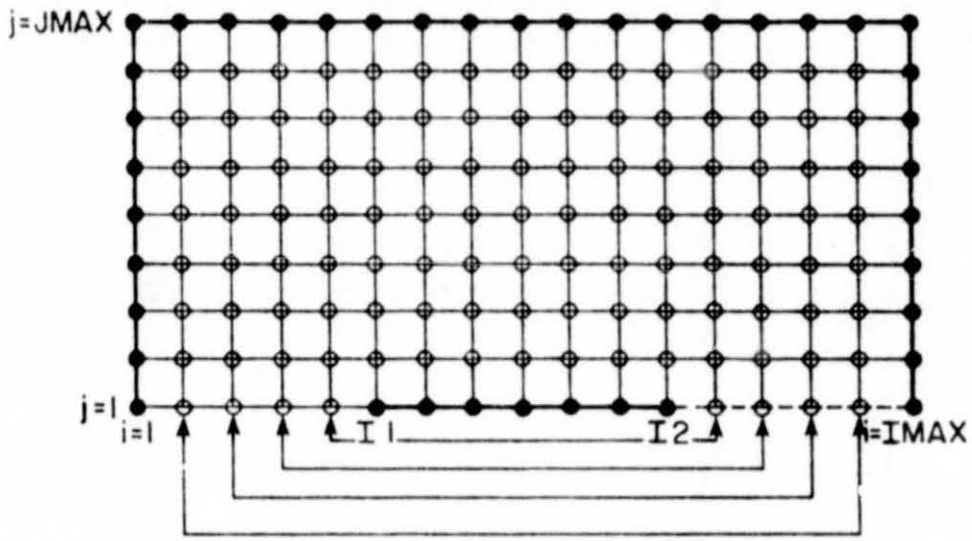

Figure 7. Computational Grid

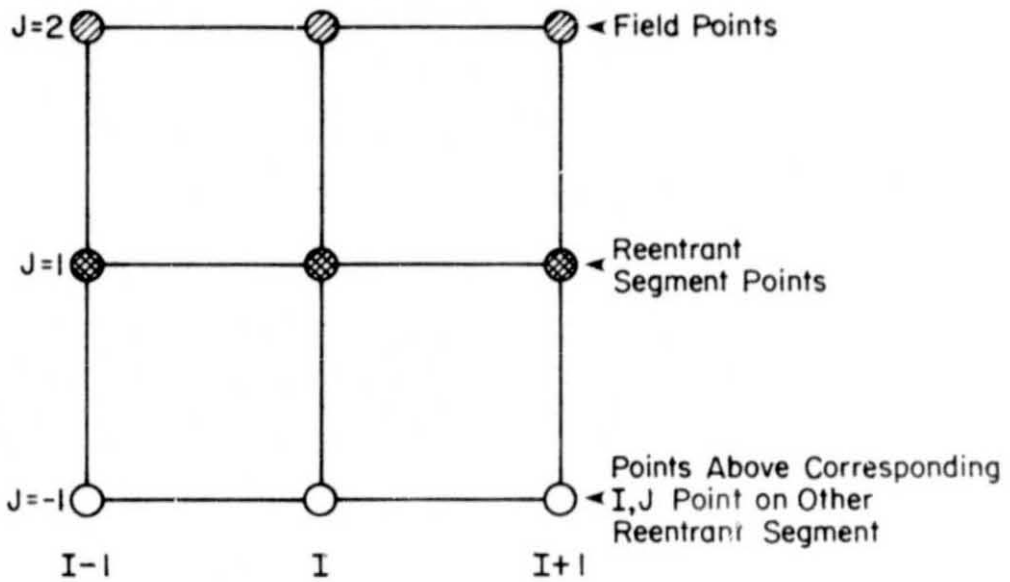

Figure 8. Section of the Computational Grid at the Cut

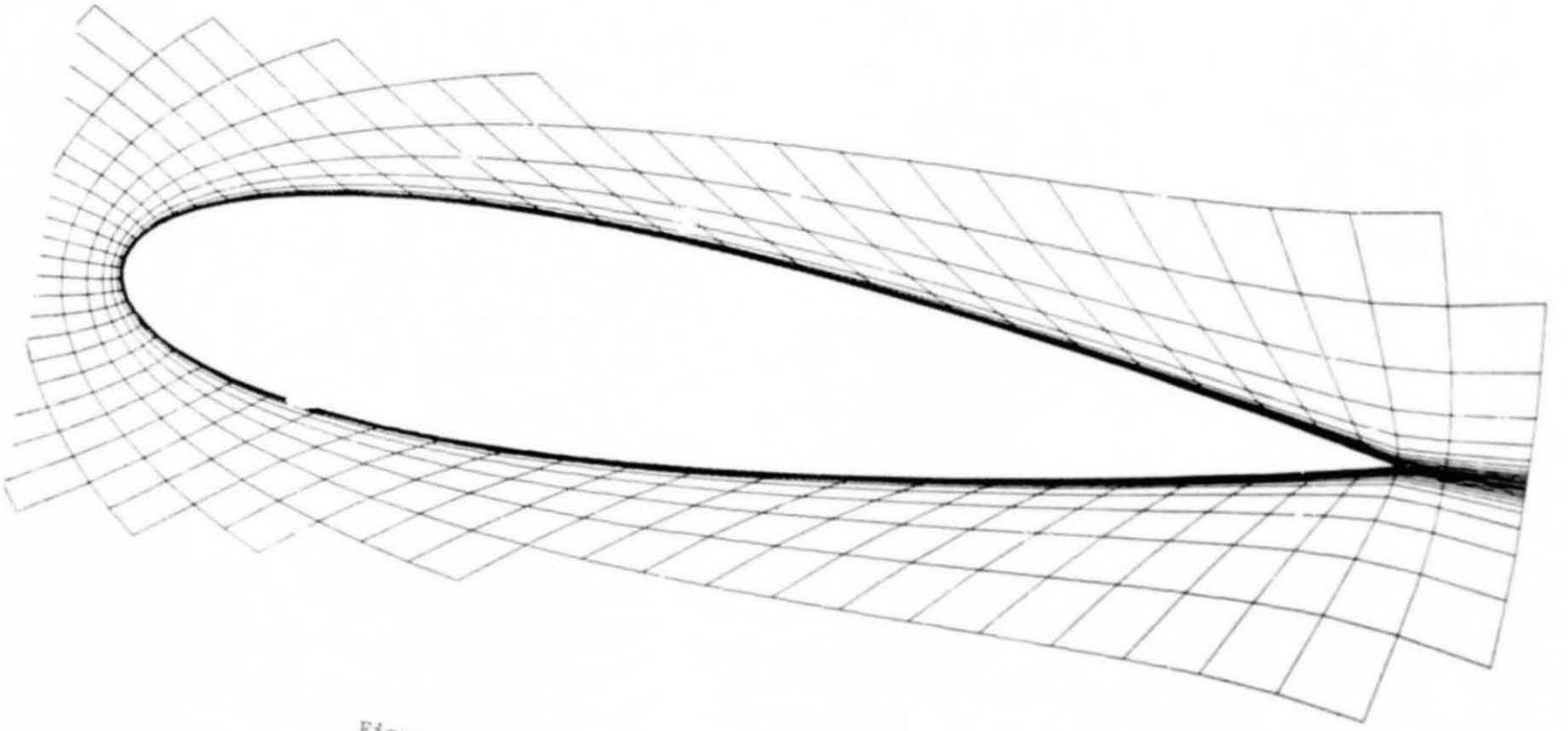

Figure 9. Detail of Coordinate System Near Airfoil

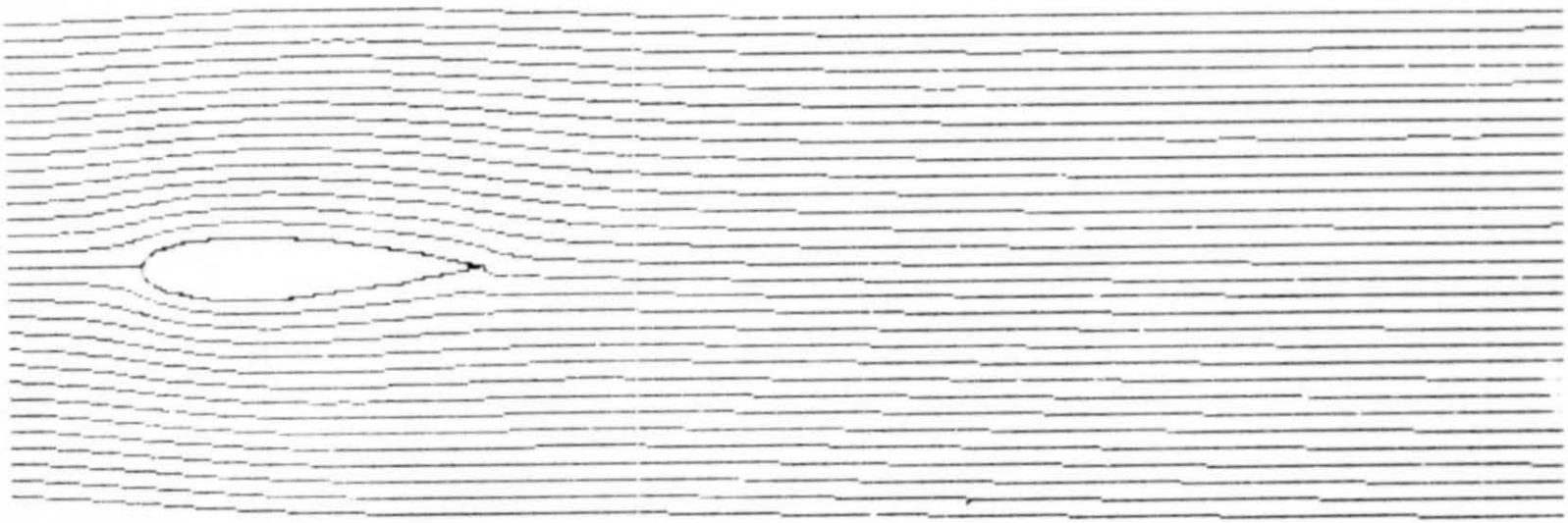

Figure 10. Streamlines (t = 1.1)

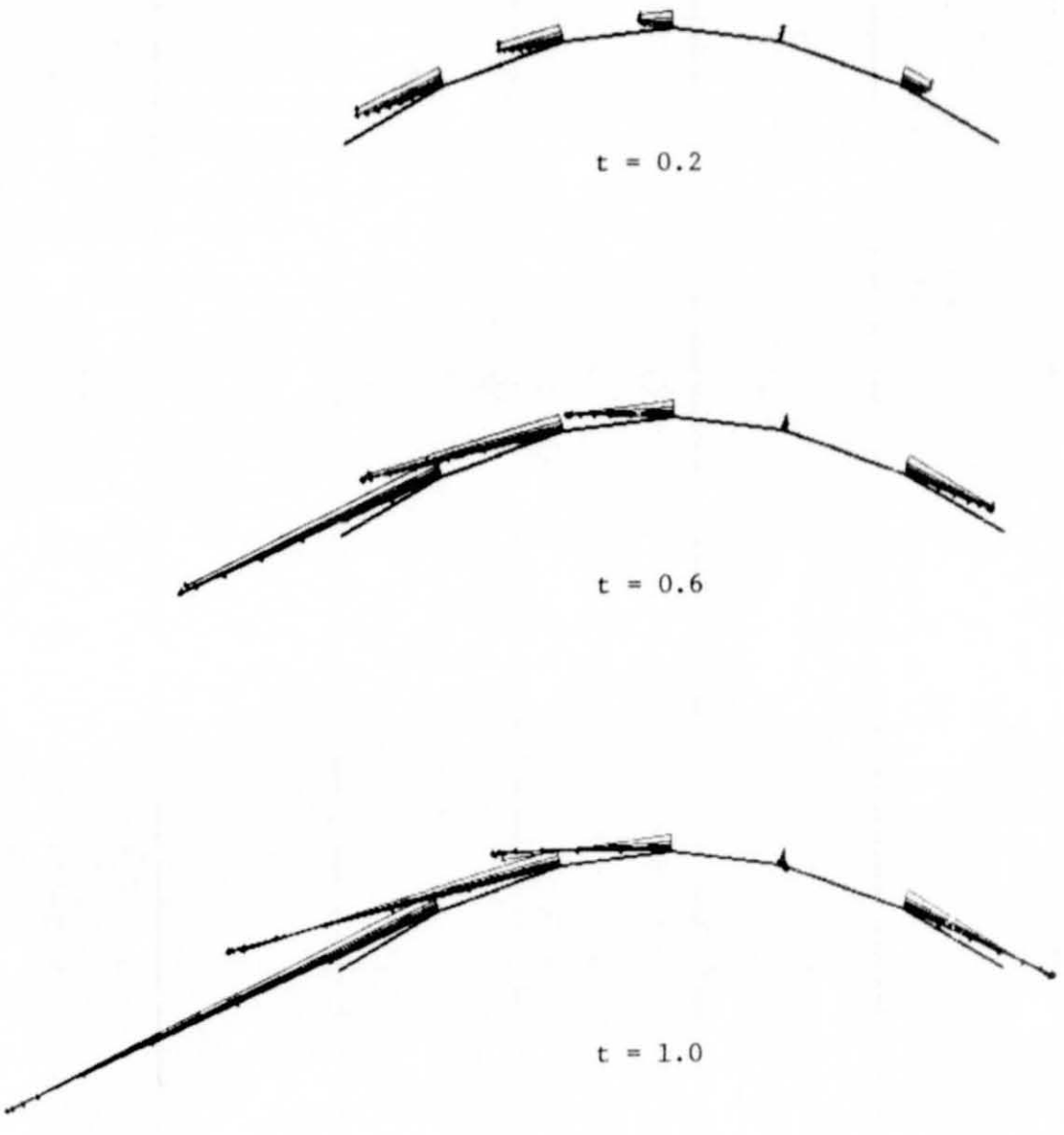

Figure 11. Velocity Profiles Near Leading Edge

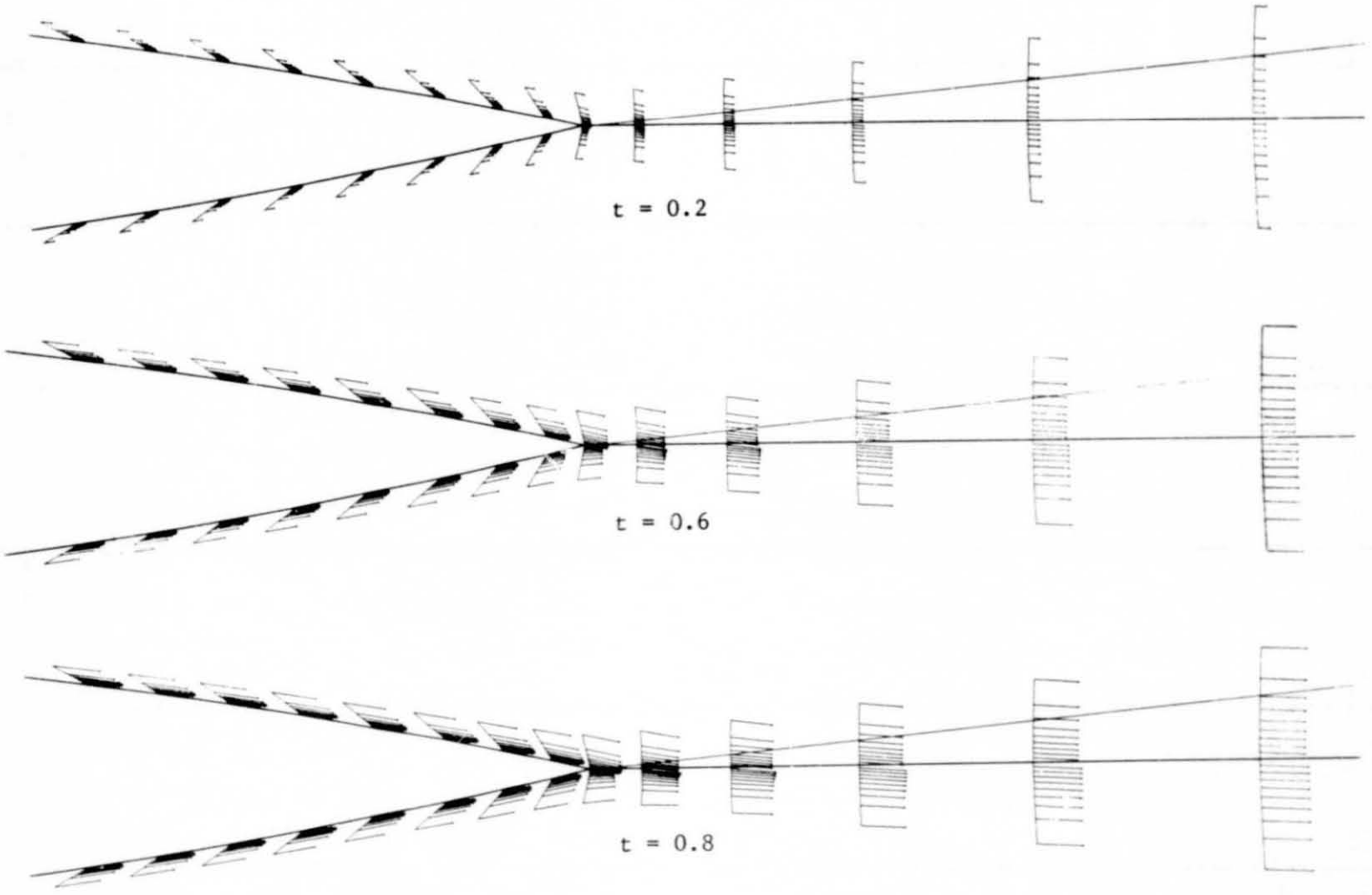

Figure 12. Velocity Profiles Near Trailing Edge

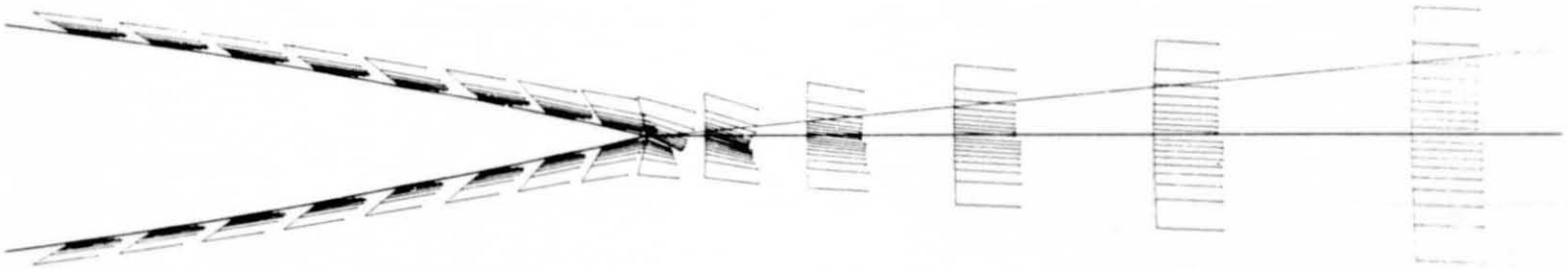

t = 1.0

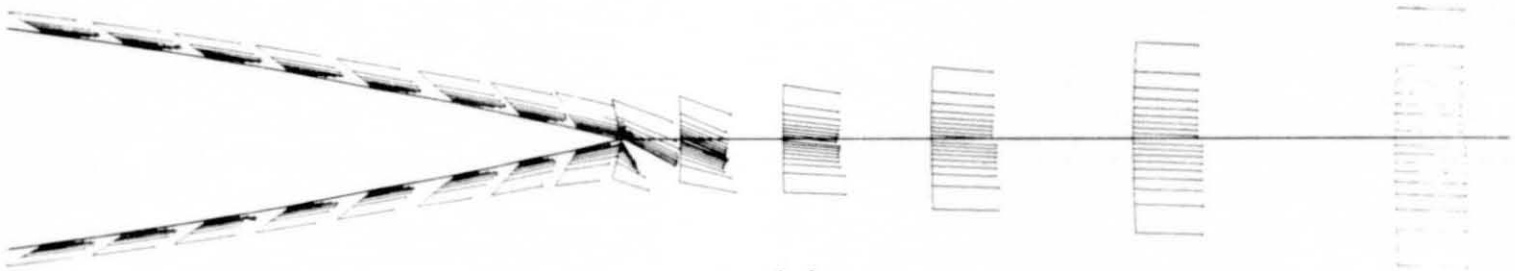

t = 1.1

Figure 12 (Cont'd)

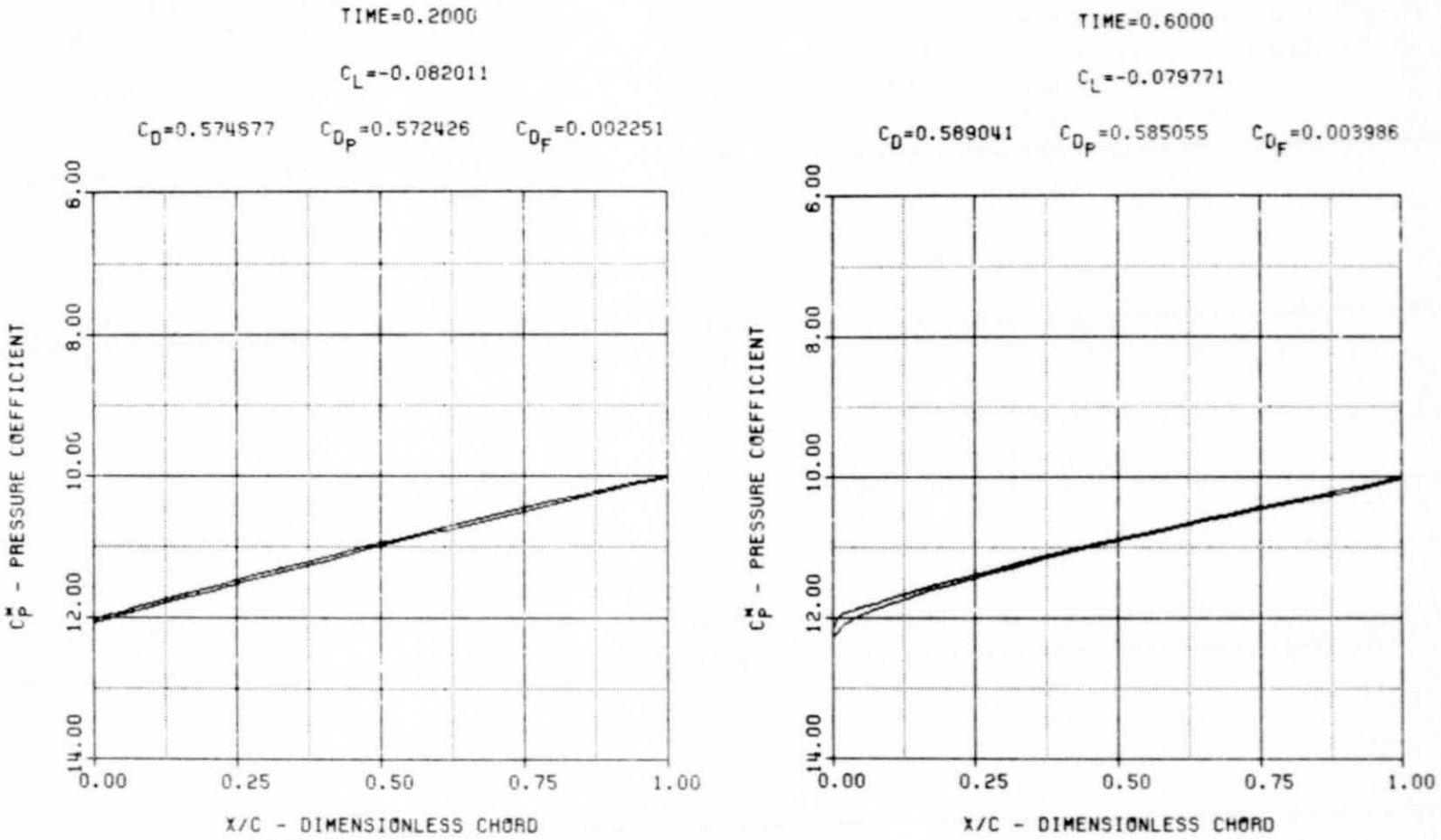

Figure 13. Pressure Distribution

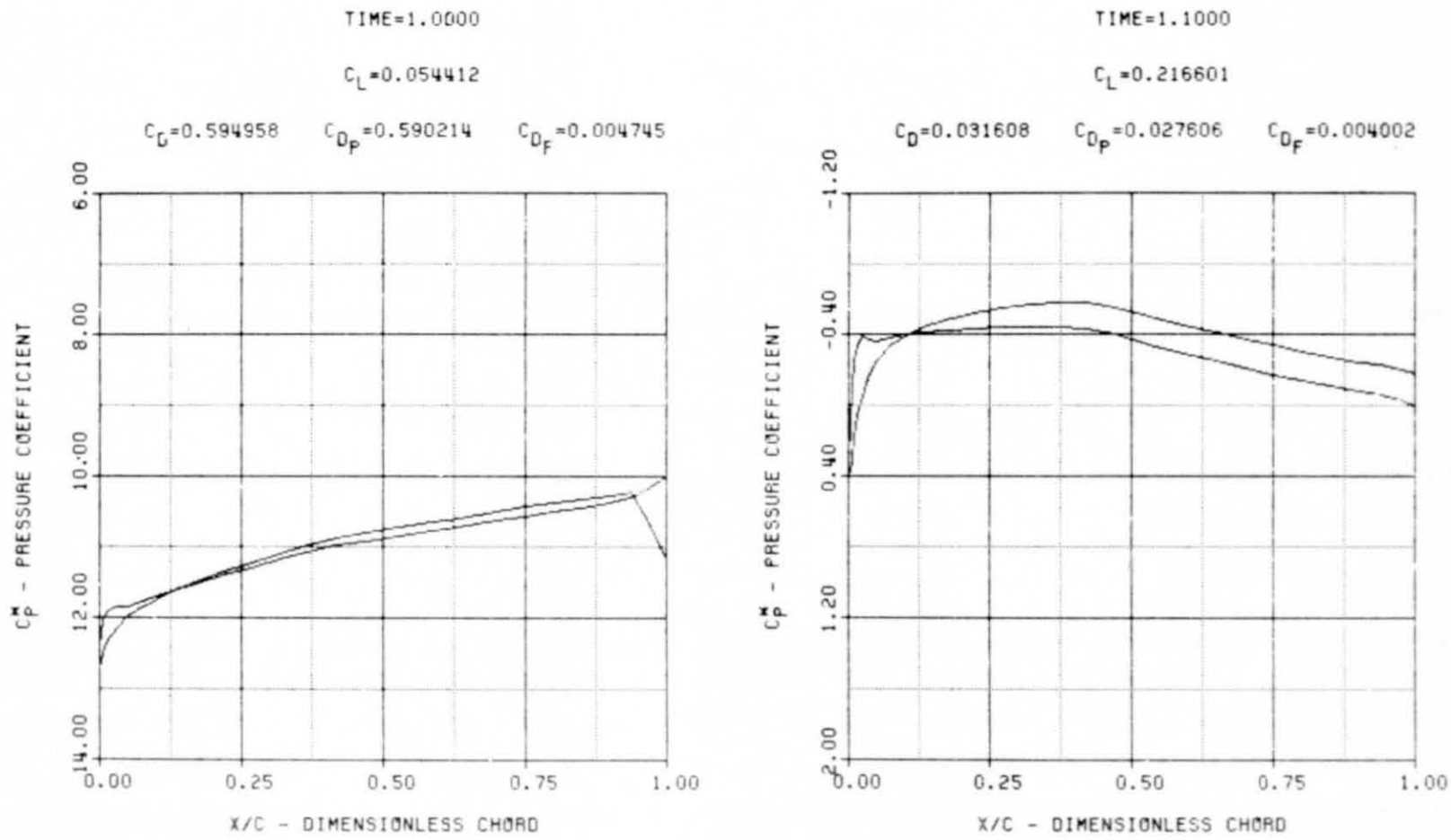

Figure 13 (Cont'd)

BIBLIOGRAPHY

1. Thames, Frank C., "Numerical Solution of the Incompressible Navier-Stokes Equations About Arbitrary Two-Dimensional Bodies," Ph.D. Dissertation, Mississippi State University, (1975).

2. Reddy, Rama N., "Numerical Solution of Incompressible Navier-Stokes Equations in Integro-Differential Formulation Using Boundary-Fitted Coordinate System," Ph.D. Dissertation, Mississippi State University, (1977).

3. Shanks, Samuel P., "Numerical Simulation of Viscous Flow about Submerged Arbitrary Hydrofoils using Non-orthogonal, Curvilinear Coordinates," Ph.D. Dissertation, Mississippi State University, Mississippi State, Mississippi, (1977).

4. Thompson, Joe F. and Warsi, Z.U.A., "Machine Solutions of Partial Differential Equations in the Numerically Generated Coordinate Systems," August 1976, pp. 2-14.

5. Thames, Frank C., et al, "Numerical Solutions for Viscous and Potential Flow about Arbitrary Two-Dimensional Bodies Using Body-Fitted Coordinate Systems," Journal of Computational Physics, Vol. 24, 1977.

6. Thompson, Joe F., Thames, Frank C., and Mastin, C. Wayne, "TOMCAT - A Code for Numerical Generation of Boundary-Fitted Curvilinear Coordinate Systems on Fields Containing Any Number of Arbitrary Two-Dimensional Bodies," Journal of Computational Physics, Vol. 24, 1977.

7. Israeli, M., "A Fast Implicit Numerical Method for Time Dependent Viscous Flows," Studies in Applied Mathematics, Vol. 49, No. 4, 1970, pp. 327-349.

8. Walker, R. L., "Numerical Solution of the Navier-Stokes Equations for Incompressible Viscous Laminar Flow Past a Semi-Infinite Flat Plate," Master's Thesis, Mississippi State University, December 1974.